

Electrical spin injection and detection in an InAs quantum well

Hyun Cheol Koo, Hyunjung Yi, Jae-Beom Ko, Joonyeon Chang,* and Suk-Hee Han
Nano Device Research Center, Korea Institute of Science and Technology, Seoul 136-791, Korea

Donghwa Jung, Seon-Gu Huh, and Jonghwa Eom†
*Department of Physics, Sejong University, Seoul 143-747, Korea and
Nano Device Research Center, Korea Institute of Science and Technology, Seoul 136-791, Korea*
(Dated: September 5, 2018)

We demonstrate fully electrical detection of spin injection in InAs quantum wells. A spin polarized current is injected from a $\text{Ni}_{81}\text{Fe}_{19}$ thin film to a two-dimensional electron gas (2DEG) made of InAs based epitaxial multi-layers. Injected spins accumulate and diffuse out in the 2DEG, and the spins are electrically detected by a neighboring $\text{Ni}_{81}\text{Fe}_{19}$ electrode. The observed spin diffusion length is $1.8 \mu\text{m}$ at 20 K. The injected spin polarization across the $\text{Ni}_{81}\text{Fe}_{19}/\text{InAs}$ interface is 1.9% at 20 K and remains at 1.4% even at room temperature. Our experimental results will contribute significantly to the realization of a practical spin field effect transistor.

PACS numbers: 72.25.Dc, 72.25.Hg, 72.25.Rb, 85.75.Hh

Spintronics is a fascinating new paradigm with the potential to overcome some of the physical limitations of conventional electronics. An essential ingredient of spintronic devices is the presence of a spin-polarized current, which is often generated by current injection from ferromagnetic metals. However, contemporary spintronics faces the challenge of developing efficient injection and detection methods for spin-polarized currents in semiconductors. In particular, fully electrical spin injection and detection are the primary prerequisites for realizing a spintronic device which is compatible with other electronic charge based devices. Here we provide a manifest evidence of the purely electrical detection of spin injection and accumulation in InAs quantum wells. Spins injected from a $\text{Ni}_{81}\text{Fe}_{19}$ thin film accumulate and diffuse out in the InAs quantum well, with the spins being electrically detected by a neighbouring $\text{Ni}_{81}\text{Fe}_{19}$ electrode. The observed spin signals provide us with substantive information such as the injected spin polarization and the spin relaxation time in the InAs quantum well over a wide temperature range up to room temperature.

We have constructed a mesoscopic semiconductor lateral spin valve that exhibits fully electrical spin injection and detection. The device consists of two ferromagnetic electrodes and an InAs high-electron-mobility transistor (InAs HEMT). The InAs HEMT has been epitaxially grown by molecular beam epitaxy on a semi-insulated InP(100) substrate. A quantum well, which functions as a two-dimensional electron gas channel (2DEG), is present at a depth of 35.5 nm from the top surface. The carrier density and mobility of 2DEG are $n = 6.3 \times 10^{12}$ (4.6×10^{12}) cm^{-2} and $\mu = 5,700$ ($34,700$) $\text{cm}^2\text{V}^{-1}\text{s}^{-1}$ at 295 K (20 K). A scanning electron micrograph of a representative device is shown in Fig. 1(a). The essential parts

of the device are a single $8\text{-}\mu\text{m}$ -wide InAs HEMT channel and two ferromagnetic electrodes that work as the spin injector and detector. The ferromagnetic electrodes have different aspect ratios, and hence exhibit distinctive magnetization-switching fields. A desired configuration of magnetization orientations can be obtained by applying the external magnetic field along the easy axis of the ferromagnetic patterns.

The most delicate step in the device fabrication process is constructing an appropriate interface between the ferromagnetic electrode and the InAs HEMT. We found that the electrical detection of spin injection was stable and reproducible only for devices with an interface resistance for which $R_{F/SC}A_J = 20\sim 50 \Omega\text{-}\mu\text{m}^2$ at 20 K, where A_J is the interface area and $R_{F/SC}$ is the resistance of the interface between the $\text{Ni}_{81}\text{Fe}_{19}$ film and the InAs HEMT. A thickness of $25.5\sim 32.5$ nm was removed from the top surface by Ar-ion milling and exposed to dry air to yield a very thin oxide layer, after which an 80-nm-thick $\text{Ni}_{81}\text{Fe}_{19}$ film was sputtered from a single target in a magnetic field. Figure 1(b) shows a schematic diagram of the cross section where the ferromagnetic electrode was deposited. The distance between the ferromagnetic layer and the InAs quantum well is $3\sim 10$ nm, as measured by transmission electron microscopy. This distance was found to be the most suitable for spin injection and detection in our experiments.

To examine the characteristics of the interface, we compared effective resistances R_F and R_{SC} of a spin diffusion length for NiFe and the InAs 2DEG, and the interface resistance $R_{F/SC}$ [1, 2, 3]. Using the values determined from this experiment, we estimate that $R_F = \rho_F \lambda_F / A_J \approx 4.0 \times 10^{-5} \Omega$ and $R_{SC} = \rho_{SC} \lambda_{SC} / A_{SC} \approx 21 \Omega$, where ρ_x and λ_x are the resistivities and the spin diffusion lengths for NiFe (“F”) and the InAs 2DEG (“SC”), respectively, and A_{SC} is the cross-sectional area of the InAs 2DEG. We used $\lambda_F = 4.3$ nm, as obtained in a previous spin-valve experiment [4]. The typical $R_{F/SC}$ required to observe spin signals in this experi-

*Electronic address: presto@kist.re.kr

†Electronic address: eom@sejong.ac.kr

ment is $1\sim 10\ \Omega$, indicating that the interface resistance is in the range $R_F \ll R_{F/SC} < R_{SC}$, which is neither transparent ($R_{F/SC} \ll R_F$) nor strictly tunnelling-like ($R_{F/SC} \gg R_{SC}$). It should be noted that the conductance-mismatch model [5] developed for the transparent limit is not applicable to the systems in this letter.

Spin injection can be detected electrically by measuring correlations of the magnetization of two ferromagnetic electrodes. Two different measurement geometries are usually employed for these measurements. The first type of measurement is the four-probe measurement in local spin-valve geometry, in which voltage drops associated with current flows between the ferromagnetic electrodes are measured, yielding the resistance in parallel (R_{par}) and antiparallel (R_{anti}) magnetization configurations. Figure 2(a) shows the magnetoresistance measured in the local spin-valve geometry. The spin-valve effect can be estimated by the relative magnetoresistance $\Delta R/R_{par} = (R_{anti} - R_{par})/R_{par}$. When the distance between ferromagnetic electrodes is much smaller than the spin relaxation length (λ_F) in the ferromagnetic electrodes, $\Delta R/R_{par}$ has the maximum value of $\beta^2/(1 - \beta^2)$, where β is the bulk spin polarization in the ferromagnetic electrode. However, the distance between the ferromagnetic electrodes is usually larger than the spin relaxation length in a conventional lateral spin-valve device, in which case the relative magnetoresistance effect has a very small magnitude. In our lateral spin-valve devices the observed $\Delta R/R_{par}$ was as small as 0.029% (Fig. 2(a)).

The second type of measurement involves nonlocal geometry, which is used to obtain the spin diffusion length in a metal or a semiconductor. In this measurement geometry, the voltage is not measured where the charge current flows; instead, only the chemical potential that is sensitive to spin accumulation is measured using a ferromagnetic detector. Figure 2(b) shows the nonlocal spin signal as a function of magnetic field applied along the easy axis of ferromagnetic patterns. The chemical potential in the parallel (antiparallel) magnetization makes an additive (subtractive) contribution to the nonlocal voltage. The ranges of magnetic fields where the resistance dips appear in the nonlocal spin signal match exactly with the ranges where the resistance maxima occur in the local spin-valve signal of Fig. 2(a). The characteristics of the observed nonlocal spin signal do not change even if the injection and detection electrodes are exchanged. Since the Hall effect is antisymmetric with respect to the zero magnetic field, it is unlikely that the signal in Fig. 2(b) contains any contribution from the Hall effect given that the baseline resistance is flat and no significant antisymmetric component was detected. For this reason, we abandoned the speculation that the Hall voltage may be detected using the nonlocal geometry.

The spin diffusion length and the injected spin polarization were estimated from an analysis of the space correlation of the nonlocal spin signal. Figure 3(a) shows the spatial dependence of the magnitude of the nonlocal spin

signal. The spatial dependence of the nonlocal spin signal $\Delta R = (R_{par} - R_{anti})$ is known to follow the exponential-decay formula $\Delta R = (\eta^2 R_s \lambda_s / w) \exp(-L/\lambda_s)$, where η is the injected spin polarization of the current crossing the NiFe-InAs interface, R_s is the sheet resistance of the InAs 2DEG, w is the width of the InAs 2DEG, λ_s is the spin diffusion length of the InAs 2DEG and L is the center-to-center distance between the ferromagnetic electrodes. Fitting the obtained data to the formula yields estimates of $\lambda_s \approx 1.8\ \mu\text{m}$ and $\eta \approx 1.9\%$ at 20 K. The black solid line in Fig. 3(a) represents the fitted curve for 20 K, and similar fits were obtained for other temperatures. We estimate that $\lambda_s \approx 1.9\ \mu\text{m}$ and $\eta \approx 1.7\%$ at 50 K, $\lambda_s \approx 1.5\ \mu\text{m}$ and $\eta \approx 1.7\%$ at 100 K, and $\lambda_s \approx 1.3\ \mu\text{m}$ and $\eta \approx 1.4\%$ at 295 K. The injected spin polarization shows a very weak dependence on temperature (Fig. 3(b)). These data represent the determination of η purely by electrical detection of spin injection in a semiconductor. Moreover, the injected spin polarization remains at 1.4% up to room temperature. This weak temperature dependence of η is consistent with a previous study in which the spin injection into a GaAs quantum well was examined by observing circularly polarized light [6].

The spin relaxation time can be estimated from $\tau_s = \lambda_s^2/D$. The diffusion constant is given by $D = 1/[N(E_F)e^2 R_s]$, where $N(E_F)$ is the density of states at the Fermi level and e is the electron charge. Figure 3(c) shows that the temperature dependence of τ_s in the InAs 2DEG is rather weak. In a previous investigation of spin relaxation using pumping-probe optical orientation spectroscopy, the temperature dependence of spin relaxation in GaAs-based quantum wells was observed to depend on the confinement energy [7]. That study showed that τ_s depends very weakly on temperature for narrow quantum wells (i.e. with a width of less than 10 nm) while it follows an inverse-square dependence with temperature for wide quantum wells. The width of our InAs quantum well was narrow (2 nm), so the weak temperature dependence of τ_s in Fig. 3(c) is consistent with spin relaxation in GaAs-based quantum wells. The temperature dependence of spin relaxation is also consistent with predictions of the D'yakonov-Kachorovski [8] and D'yakonov-Perel [9] mechanisms that the spin relaxation rate $1/\tau_s$ scales as $T^3\tau_p$ in a bulk semiconductor and a wide quantum well, and as $TE_1^2\tau_p$ in a narrow quantum well, where E_1 is the confinement energy of the quantum well, τ_p is the momentum scattering time and T is the temperature. Therefore, τ_s of the narrow quantum well (as in our InAs HEMT) is expected to be independent of T when τ_p is inversely proportional to T . For comparison we have also estimated τ_p of the InAs HEMT from measurements of the sheet resistance and the Hall effect. In the temperature range of our experiment, τ_p was roughly inversely proportional to T (Fig. 3(c)).

Purely electrical spin injection and detection in a semiconductor are important prerequisites for constructing a spin-FET. In the model spin-FET proposed by Datta and

Das [10], spins injected from a ferromagnetic electrode reach the other ferromagnetic electrode after precession due to the Rashba interaction that occurs in a semiconductor channel. Since the strength of the Rashba spin-orbit interaction is modulated by the gate electrode in the spin-FET, the output signal is modified by changes in the spin precession angle. Realizing a spin-FET requires a semiconductor with a controllable α . Our layer

structure is very similar to a previously reported inverted InGaAs/InAlAs heterostructure with controllable α by a gate voltage [11]. Consequently, the results in this letter will contribute significantly to the realization of a practical spin-FET.

This work was supported by the KIST Vision 21 Program.

-
- [1] M. Johnson, and R. H. Silsbee, Phys. Rev. B **35**, 4959 (1987).
 [2] E. I. Rashba, Phys. Rev. B **62**, R16267 (2000).
 [3] S. Takahashi and S. Maekawa, Phys. Rev. B **67**, 052409 (2003).
 [4] S. Dubois, L. Piraux, J. M. George, K. Ounadjela, J. L. Duvail, and A. Fert, Phys. Rev. B **60**, 477 (1999).
 [5] G. Schmidt, D. Ferrand, L. W. Molenkamp, A. T. Filip, and B. J. van Wees, Phys. Rev. B **62**, R4790 (2000).
 [6] A. T. Hanbicki, B. T. Jonker, G. Itskos, G. Kioseoglou, and A. Petrou, Appl. Phys. Lett. **80**, 1240 (2002).
 [7] A. Malinowski, R. S. Britton, T. Grevatt, R. T. Harley, D. A. Ritchie, and M. Y. Simmons, Phys. Rev. B **62**, 13034 (2000).

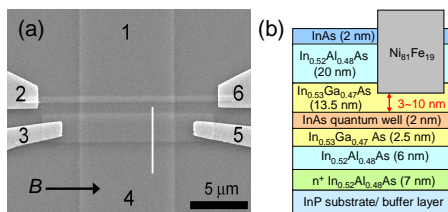


FIG. 1: (a) Scanning electron micrograph of the mesoscopic ferromagnet-semiconductor spin-valve device. An $8\text{-}\mu\text{m}$ -wide two-dimensional electron gas channel, which is connected by terminals 1 and 4, is defined by dry etching. The external magnetic field, B , is applied along the easy axis of the ferromagnetic film. The white line represents a cut line for the cross-sectional view. (b) Schematic of the cross section where the ferromagnetic electrode was deposited. The buffer layer consists of 300-nm -thick $\text{In}_{0.52}\text{Al}_{0.48}\text{As}$ on top of InP substrate.

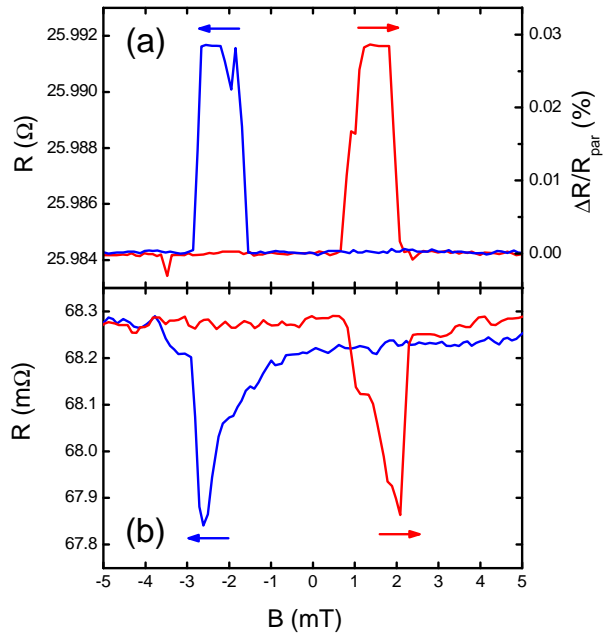


FIG. 2: (a) Magnetoresistance measured in the local spin-valve geometry at 20 K. When the current flows from terminals 2 to 3, the voltage is measured between terminals 6 and 5. The arrows represent the sweep direction of the magnetic field for each trace. (b) Nonlocal spin signal at 20 K. The nonlocal voltage is measured between terminals 3 and 4, while the current flows from terminal 2 to 1. The data were taken for the device of $L = 2.2 \mu\text{m}$. For this device, the distance between the ferromagnetic layer and the InAs quantum well is ~ 3 nm.

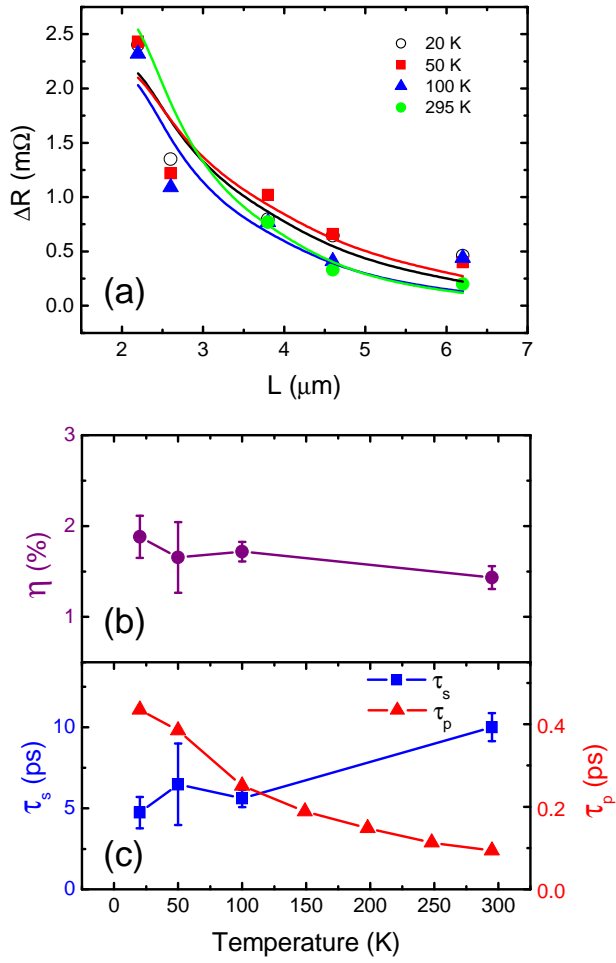


FIG. 3: (a) Spatial dependence of the magnitude of the non-local spin signal. (b) Temperature dependence of the injected spin polarization, η . (c) Temperature dependence of spin relaxation time (τ_s) and momentum scattering time (τ_p). The error bars indicate the standard deviations in our measurements. The distance between the ferromagnetic layer and the InAs quantum well of all the devices is ~ 7 nm.